NMR($CDCl_3$) δ; 1.92 (3H, s, C^9-CH_3), 3.28 (3H, s, N^1-CH_3), 5.75 (1H, s, H-10), 5.94-6.00 (2H, m, H-7 and H-8), 6.06 (1H, dd, *J*=10.9, 3.5 Hz, H-6), 6.18 (1H, d, *J*=10.9 Hz, H-5), 8.43 (1H, brs, N^3-H). NOE; H-10 with N^1-CH_3, C^9-CH_3; C^9-CH_3 with H-10, H-8; H-6 with H-7, H-5; N^1-CH_3 with H-10. ^{13}C-NMR ($CDCl_3$) δ; δ; 23.90 (C^9-CH_3), 31.91 (N^1-CH_3), 111.13 (4a), 120.60 (10), 127.13 (5), 131.14 (8), 132.21 (6), 133.07 (7), 146.29 (9), 150.87 (10a), 151.15 (2), 161.69 (4). MS *m/z* (%):216 (M^+, 100), 201 (13), 176 (5), 173 (30), 158 (11), 130 (24), 115 (11), 104 (15). HRMS; Calcd for $C_{12}H_{12}N_2O_2$: 216.0899. Found: 216.0903.

1,10-Dimethylcyclooctapyrimidine-2,4-dione($4b_{10}$): Orange oil. ^{1}H-NMR($CDCl_3$) δ; 1.94 (3H, s, C^{10}-CH_3), 3.27 (3H, s, N^1-CH_3), 5.96 (1H, dd, *J*=10.9, 3.5 Hz, H-7), 6.02 (2H, m, H-8 and H-9), 6.06 (1H, dd, *J*=10.9, 2.3 Hz, H-6), 6.28 (1H, d, *J*=10.9 Hz, H-5). NOE; C^{10}-CH_3 with N^1-CH_3, H-9; H-6 with H-5, H-7; N^1-CH_3 with C^{10}-CH_3. ^{13}C-NMR ($CDCl_3$) δ; 21.68 (C^{10}-CH_3), 32.62 (N^1-CH_3), 110.51 (4a), 126.38 (5), 130.40 (8), 132.01 (7), 132.09 (9), 132.35 (6), 133.82 (10), 151.75 (10a), 153.90 (2), 161.88 (4). MS *m/z* (%):216 (M^+, 100), 201 (17), 176 (6), 173 (32), 158 (28), 145 (37), 115 (14), 104 (23). HRMS; Calcd for $C_{12}H_{12}N_2O_2$: 216.0899. Found: 216.0899.

1,7,10-Trimethylcyclooctapyrimidine-2,4-dione(4c): Colorless crystals. mp 245-247 °C (*i*-PrOH). ^{1}H-NMR((acetone-d_6)) δ; 1.68 (3H, s, C^7-CH_3), 1.91 (3H, s, C^{10}-CH_3), 3.19 (3H, s, N^1-CH_3), 5.81 (1H, m, H-8), 5.91 (1H, brd, *J*=11.5 Hz, H-6), 6.00 (1H, m, H-9), 6.12 (1H, d, *J*=11.5 Hz, H-5). NOE; H-9 with C^{10}-CH_3, H-8; C^7-CH_3 with H-8, H-6; H-6 with C^7-CH_3, H-5; N^1-CH_3 with C^{10}-CH_3. ^{13}C-NMR ($CDCl_3$) (acetone-d_6) δ; 20.65 (C^{10}-CH_3), 22.25 (C^7-CH_3), 31.85 (N^1-CH_3), 109.89 (4a), 125.42 (5), 125.87 (8), 132.42 (9),133.23 (10), 134.22 (6), 139.57 (7), 151.50 (2), 153.82 (10a), 161.44 (4). MS *m/z* (%):230 (M^+, 100), 215 (27), 190 (19), 187 (13), 144 (37), 129 (6). *Anal.* Calcd for $C_{13}H_{14}N_2O_2$ C, 67.81; H, 6.13; N, 12.17. Found: C, 67.66; H, 6.13; N, 12.15.

9,11-Diaza-3,9-dimethyl-6-methylenepentacyclo[6.4.0.0^{1,3}.0^{2,5}.0^{4,8}]dodecane-10,12-dione(5c): colorless crystals. mp 215-217 °C (*i*-PrOH). ^{1}H-NMR ($CDCl_3$) δ; 1.48 (3H, s, C^3-CH_3), 2.45 (1H, dt, *J*=16.9, 2.6 Hz, H-7b), 2.55 (1H, dt, *J*=16.9, 2.0 Hz, H-7a), 2.80(1H, t, *J*=4.6 Hz, H-4), 2.86 (1H, dd, *J*=4.6, 2.9 Hz,H-2), 2.96 (3H, s, N^9-CH_3), 3.68 (1H, dd, *J*=4.6, 2.9 Hz, H-5), 4.75 (1H, brs, C^6=CHb), 4.91 (1H, t-like, C^6=CHa), 7.48 (1H, brs, N^{11}-H). NOE; H-2 with H-5, C^3-CH_3; H-4 with C^3-CH_3, N^9-CH_3, H-5; H-5 with H-7a, H-7b, H-6b; H-6b with H-5, H-6a; H-6a with H-6b, H-7a; H-7a with H-6b, H-7b; H-7b with H-7a, N^9-CH_3 ; N^9-CH_3 with H-7b. ^{13}C-NMR ($CDCl_3$) δ; 10.58(C3-CH_3), 29.37(N9-CH_3), 32.4(3), 34.80 (2), 47.29 (1), 50.60 (4), 51.38 (5), 68.62 (8), 107.37 (C^6=CH_2), 147.07 (6), 154.11 (10), 167.10 (12). MS *m/z* (%):229 ([M-H]$^+$, 82), 215 (69), 190 (100), 172 (20), 158 (33),147 (75),144 (38), 129 (13), 119 (89), 91 (29). HRMS; Calcd for $C_{13}H_{13}N_2O_2$; 229.0977. Found; 229.0980.

9,11-Diaza-2,9-dimethyl-5-methylenepentacyclo[6.4.0.0^{1,3}.0^{2,6}.0^{4,8}]dodecane-10,12-dione (6c): colorless crystals. mp 172-174 °C (acetone-hexane).^{1}H-NMR ($CDCl_3$) δ; 1.57 (1H, d, *J*=9.8 Hz, H-7a), 1.62 (3H, s, C^2-CH_3), 1.75 (1H, dt, *J*=9.8, 2.3 Hz, H-7b), 2.70 (1H, brt, H-6), 2.80 (1H, t, *J*=2.3, 2.9 Hz, H-4), 2.86 (3H, s, N^9-CH_3), 2.89 (1H, d, *J*=2.9 Hz ,H-3), 4.53 (1H, s, C^5=CHb),4.64 (1H, s, C^5=CHa). NOE; C^2-CH_3 with H-6, H-3; H-4 with H-3, H-5b; H-5a with H-5b; H-6 with H-5a, H-7a , C^2-CH_3 ; H-7a with H-7b; H-7b with H-7a, N^9-CH_3; N^9-CH_3 with H-7b. ^{13}C-NMR ($CDCl_3$) δ; 12.43 (C^2-CH_3), 29.37 (N^9-CH_3), 40.17 (2), 41.76 (3), 45.78 (7), 46.21 (6), 46.25 (4), 48.67 (1), 65.86 (8), 98.45 (C^5=CH_2), 152.37 (10), 157.34 (5), 167.81 (12). MS *m/z* (%):230 (M^+, 7), 215 (100), 172 (59), 144 (26), 129 (5), 115 (9), 91 (18), 77 (9). HRMS; Calcd for $C_{13}H_{14}N_2O_2$; 230.1055. Found; 230.1055.

1, 6, 8, 10-Tetramethylcyclooctapyrimidine-2, 4-dione (4d): orange oil. ^{1}H-NMR (C_6D_6) δ; 1.79 (3H, s, C^8-CH_3), 1.81 (3H, s, C^6-CH_3), 1.90 (3H, s, C^{10}-CH_3), 3.27 (3H, s, N^1-CH_3), 5.61 (1H, s, H-7), 5.95 (1H, s, H-5), 5.97 (1H, s, H-9), 9.20 (1H, brs, N^3-H). NOE; C^{10}-CH_3 with N^1-CH_3, H-9; H-9 with C^{10}-CH_3, C^8-CH_3; C^8-CH_3 with H-9, H-7; C^6-CH_3 with H-7 H-5; N^1-CH_3 with C^{10}-CH_3 .^{13}C-NMR (C_6D_6) δ; 21.37 (C^{10}-CH_3), 22.55 (C^8-CH_3), 23.78 (C^6-CH_3), 32.52 (N^1-CH_3), 112.09 (4a), 120.07 (5), 129.91 (7), 131.76 (10), 135.21 (9), 137.22 (8), 142.06 (6), 151.97 (10a), 152.93 (2), 160.89 (4). MS *m/z* (%): 244 (M^+, 100), 229 (76), 201 (5), 186 (45), 173 (23), 158 (35), 144 (15), 129 (10). HRMS; Calcd for $C_{14}H_{16}N_2O_2$; 244.1212. Found; 244.1209.

9,11-Diaza-2,4,9-trimethyl-6-methylenepentacyclo[6.4.0.0^{1,3}.0^{2,5}.0^{4,8}]dodecane-10,12-dione (5d): colorless crystals. mp 231-233 °C (EtOH).^{1}H-NMR ($CDCl_3$) δ; 1.16 (3H, s, C^4-CH_3), 1.57 (3H, s, C^2-CH_3), 2.49 (1H, dt, *J*=16.7, 2.5 Hz, H-7b), 2.58 (1H, dt, *J*=16.7, 2.5 Hz, H-7a), 2.94 (3H, s, N^9-CH_3), 2.96 (1H, s, H-5), 3.33 (1H, s, H-3), 4.84 (1H, brs, C^6=CHb), 4.93 (1H, t, *J*=2.5 Hz, C^6=CHa), 7.32 (1H, brs, N^{11}-H). NOE; C^2-CH_3 with H-5, H-3; H-3 with C^2-CH_3, C^4-CH_3; C^4-CH_3 with H-3, H-5, N^9-CH_3; H-6a with H-6b, N^9-CH_3 ; N^9-CH_3 with H-7a, C^4-CH_3. ^{13}C-NMR ($CDCl_3$) δ; 11.10 (C^2-CH_3), 14.44 (C^4-CH_3), 30.24 (1), 30.44 (N^9-CH_3), 34.99 (7), 38.74 (2), 44.78 (3), 56.46 (4), 62.63 (5), 70.77 (8), 108.31 (C^6=CH_2), 145.03 (6), 154.42 (10), 168.04 (12). MS *m/z* (%):243 ([M-H]$^+$, 13), 229 (100), 204 (24), 186 (29), 172 (20), 158 (45), 133 (29), 117 (18). HRMS; Calcd for $C_{14}H_{16}N_2O_2$; 244.1212. Found; 244.1194.

9, 11-Diaza-3, 7, 9-trimethyl-5-methylenepentacyclo[6.4.0.0^{1,3}.0^{2,6}.0^{4,8}]dodecane-10, 12-dione (6d): colorless crystals. mp 181-183 °C (acetone-hexane).^{1}H-NMR ($CDCl_3$) δ; 0.84 (3H, d, *J*=6.3 Hz, C^7-CH_3), 1.41 (3H, s, C^3-CH_3), 1.97 (1H, brq, *J*=6.3 Hz, H-7), 2.64 (1H, m,H-6), 2.74 (1H, m, H-2), 2.81 (3H, s, N^9-CH_3), 2.94 (1H, s, H-4), 4.50 (1H, s, C^5=CHa), 4.61 (1H, s, C^5=CHb). NOE; C^3-CH_3 with H-2, H-6 ; H-5a with H-6 , H-5b; H-5b with H-5a, H-6; H-6 with H-5a, H-5b, H-4, H-2, N^9-CH_3,

C^3-CH_3, C^7-CH_3; C^7-CH_3 with H-7, H-6, N^9-CH_3; N^9-CH_3 with H-6, H-7. ^{13}C-NMR ($CDCl_3$) δ; 8.43 (C^7-CH_3), 12.62 (C^3-CH_3), 29.60 (N^9-CH_3), 39.83 (2), 46.61 (6), 47.83 (3), 50.52 (4), 50.65 (1), 51.36 (7), 66.31 (8), 98.35 (C^5=CH_2), 153.13 (10), 156.44 (5), 167.21 (12). MS *m/z* (%):244 (M^+, 56), 229 (100), 201 (14), 200 (11), 186 (51), 173 (9), 158 (39), 144 (9), 129 (12), 116 (8). HRMS; Calcd for $C_{14}H_{16}N_2O_2$; 244.1212. Found; 244.1216.

ACKNOWLEDGMENTS

This work has been supported in part by "Academic Frontier" Project from the Ministry of Education, Culture, Sports, Science and Technology of Japan.

REFERENCES

1. M. D. Shetlar, *Photochem. Photobiol. Rev.*, 1980, **5**, 105; T. Matsuura, I. Saito, H. Sugiyama, and T. Shinmura, *Pure Appl. Chem.*, 1980, **52**, 2705.
2. K. Seki, N. Kanazashi, and K. Ohkura, *Heterocycles*, 1991, **32**, 229; K. Ohkura, K. Kanazashi, and K. Seki, *Chem. Pharm. Bull.*, 1993, **41**, 239.
3. K. Ohkura, Y. Noguchi, and K. Seki, *Heterocycles*, 1997, **46**, 141; K. Ohkura, Y. Noguchi, and K. Seki, *Heterocycles*, 1998, **47**, 429; K. Ohkura, Y. Noguchi, and K. Seki, *Heterocycles*, 1998, **49**, 59.
4. K. Ohkura, K. Nishijima, A. Sakushima, and K. Seki, *Heterocycles*, 2000, **53**, 1247; K. Ohkura, K. Nishijima, S. Uchiyama, A. Sakushima, and K. Seki, *Heterocycles*, 2001, **54**, 65; K. Ohkura, K. Nishijima, S. Uchiyama, A. Sakushima, and K. Seki, *Heterocycles*, 2001, **55**, 1015.
5. K. Ohkura and K. Seki, *Photochem. Photobiol.*, 2002, **75**, 579.
6. K. Ohkura, N. Kanazashi, K. Okamura, T. Date, and K. Seki, *Chem. Lett.* **1993**, 667; K. Ohkura, K. Seki, H. Hiramatsu, K. Aoe, M. Terashima, *Heterocycles*, 1997, **44**, 467.
7. K. Ohkura, K. Nishijima, and K. Seki, *Chem. Pharm. Bull.*, 2001, **49**, 384; K. Ohkura, K. Nishijima, and K. Seki, *Photochem. Photobiol.*, 2001, **74**, 385.

Available online at www.sciencedirect.com
SCIENCE DIRECT
Tetrahedron Letters
Tetrahedron Letters 47 (2006) 5321–5323

A new convenient method for the synthesis of [2-^{11}C]thymine utilizing [^{11}C]phosgene

Kazue Ohkura,[a,*] Ken-ichi Nishijima,[a] Kimihito Sanoki,[a] Yuji Kuge,[b] Nagara Tamaki[b] and Koh-ichi Seki[b,*]

[a]*Faculty of Pharmaceutical Sciences, Health Sciences University of Hokkaido, Ishikari-Tobetsu, Hokkaido 061-0293, Japan*
[b]*Graduate School of Medicine, Hokkaido University, Kita-15, Nishi-7, Kita-ku, Sapporo 060-8638, Japan*

Received 4 April 2006; revised 18 May 2006; accepted 19 May 2006
Available online 13 June 2006

Abstract—β-(*N*-Benzoylamino)methacrylamide, a key intermediate for the preparation of [2-^{11}C]thymine, was synthesized in three steps from ethyl α-formylpropionate and NH_3. Reaction of the alkali metal salts of β-(*N*-benzoylamino)methacrylamide with [^{11}C]phosgene gave [2-^{11}C]thymine. The yield of [2-^{11}C]thymine was 362 ± 53 MBq at EOS ($n = 3$) (18 MeV proton beam; 10 μA, 10 min). The total synthesis was accomplished in just 16 min from the end of bombardment.

Uracil derivatives are of considerable interest because of their wide array of pharmacological properties, and many pyrimidine-based radiopharmaceuticals have been developed for clinical diagnosis in the field of single photon or positron emission computed tomography.[1] The search for new or improved synthetic routes leading to labeled thymidine for evaluation of cellular proliferation by positron emission tomography (PET) has attracted much attention in recent years. Because of the short-lived positron emitting radionuclide (ca. ^{11}C: 20.4 min, ^{13}N: 10.0 min, ^{15}O: 2.0 min, respectively) and the radioactive level, a very rapid and simple labeling process with an efficient organic reaction and an automated synthesis apparatus to avoid radiation exposure are essential conditions for PET radiotracer synthesis.

In 1991, Vander Borght et al. synthesized [2-^{11}C]thymidine from [2-^{11}C]thymine formed via cyclocondensation of diethyl β-methyl malate with [^{11}C]urea.[2] Although other investigators have attempted to improve this method or develop related methodologies, the key ring closure reactions have traditionally relied on the condensation of a malate intermediate with the labeling agent [^{11}C]urea derived from phosgene,[2,3] cyanide,[4] or carbon dioxide.[5] Typically the reactions are carried out under as drastic conditions as those employed for ^{14}C labeled thymine synthesis.[6] The complexity of the currently available synthetic routes along with the extended length of preparation time has limited the extensive applicability of ^{11}C labeled nucleosides in PET studies.

Recently, we have developed a simplified and highly efficient synthesis of [^{11}C]$COCl_2$ with high specific activity.[7] ^{11}C labeled phosgene is a high-potency agent for the introduction of a ^{11}C carbonyl group to form versatile heterocyclic compounds as well as a variety of ureas. We have explored the utility of [^{11}C]$COCl_2$ for producing high-specific activity [^{11}C]CGP-12177, a radioligand for β-adrenoreceptors in the field of clinical PET.[8] This work has now prompted us to apply [^{11}C]$COCl_2$ in a ring closure step that would provide an efficient synthesis of [2-^{11}C]thymine.

We have designed alternative precursors as sources for the carbon skeleton that can be cyclocondensed with [^{11}C]$COCl_2$ to form the desired [2-^{11}C]thymine. Our strategy for the synthesis of [2-^{11}C]thymine is depicted in Scheme 1, wherein the key intermediate is β-aminomethacrylamide derivative (**1**). We now report herein a facile synthesis of [2-^{11}C]thymine by the direct condensation of [^{11}C]$COCl_2$ with the novel intermediate (**1**).

Keywords: [^{11}C]phosgene; [2-^{11}C]thymine; Positron emission tomography; β-(*N*-Benzoylamino)methacrylamide.
Abbreviations: EOS, end of synthesis; EOB, end of bombardment; PET, positron emission tomography; DME, 1,2-dimethoxyethane.
* Corresponding authors. Tel./fax: +81 1332 3 1267 (K.O.); e-mail: ohkura@hoku-iryo-u.ac.jp

0040-4039/$ - see front matter © 2006 Elsevier Ltd. All rights reserved.
doi:10.1016/j.tetlet.2006.05.143

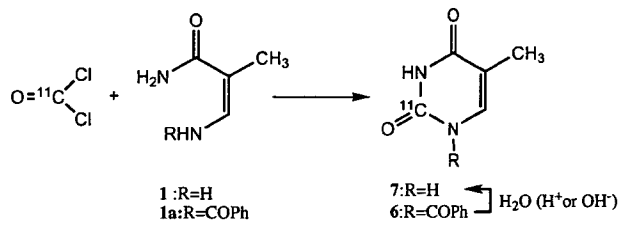

Scheme 1. Synthetic route of [2-^{11}C]thymine.

We have attempted to prepare the novel precursor β-aminomethacrylamide derivative (**1**), which leads to thymine or 1-acylated thymines by condensation reaction with phosgene. Previously, it had been reported that 1-acetylated or benzoylated thymine derivatives are rapidly hydrolyzed in ca. 20 s to produce thymine (Scheme 1).[9]

The key intermediate (**1**) was synthesized from β-aminomethacrylate (**3**) formed by the reaction of ethyl α-formylpropionate (**2**)[10] with NH_3. With the intent to activate the ester for producing amide, **3** was benzoylated prior to treatment with NH_3.

Treatment of the resulting compound (**4**) with NH_3 exclusively afforded β-(*N*-benzoylamino)methacrylamide (**1a**) without any detectable formation of the hydrolyzed product β-aminomethacrylamide (**1**, R = H) (Scheme 2). Attempts at the hydrolysis of benzoylated compound (**1a**) did not give **1**, hence, we examined the ring closure reaction using β-(*N*-benzoylamino)methacrylamide (**1a**).[11]

Synthesis of cold thymine was examined with **1a** by using triphosgene, which can be easily handled as a safe and stable replacement for phosgene. In order to accomplish the desired cyclocondensation, **1a** was activated as its alkali-metal salt. Addition of triphosgene to the sodium salt in DMF followed by hydrolysis gave thymine quantitatively.[12]

^{11}C labeled thymine production was achieved by using the same automated synthesis system as used for [^{11}C]CGP production from [^{11}C]$COCl_2$.[8] [^{11}C]$COCl_2$ was synthesized from [^{11}C]methane via [^{11}C]CCl_4 according to our previously reported method.[7] [^{11}C]methane was produced using an ultracompact cyclotron by the ^{14}N (p, α) ^{11}C nuclear reaction on nitrogen containing hydrogen (5%) in an aluminum target. Bombardment was carried out with a 10 μA beam of 18 MeV protons for 10 min.

The direct ring closure reaction of [^{11}C]$COCl_2$ possessing superior reactivity with non-activated precursor (**1a**) was first examined, but this approach failed to give the target product. Thymine precursor (**1a**), which was activated as the alkali metal salt (**5a,b**) reacted with [^{11}C]$COCl_2$ as well as triphosgene to afford [2-^{11}C]thymine (Scheme 3). The best result was obtained when the reaction was performed with potassium salt (**5b**) in DME as shown in Table 1.[13] The yield of [2-^{11}C]thymine under these conditions was 362 ± 53 MBq at EOS ($n = 3$). The radiochemical yield of [2-^{11}C]thymine was ca. 27% from [^{11}C]$COCl_2$.[14] The [2-^{11}C]thymine produced was identified by co-chromatography with authentic thymine and found to be radiochemically homogeneous by HPLC. Additionally, it was confirmed by subsequent enzymatic conversion to [2-^{11}C]thymidine.[3,15] Thus our method, which utilizes the reaction of [^{11}C]$COCl_2$ with the appropriate activated precursor is a viable approach to providing an adequate supply of [2-^{11}C]thymine, reliably and reproducibly, for clinical PET tracer studies with [2-^{11}C]thymidine.

In all previous reports, labeling of the 2-position of thymine was accomplished by condensation of [^{11}C]urea and malate at 130 °C in fuming sulfuric acid. Recently, Steel et al. reported an improved method for the preparation of [2-^{11}C]thymine via a multi-step process using [^{11}C]urea derived from [^{11}C]$COCl_2$. This radiosynthesis of [2-^{11}C]thymine took approximately 30 min from EOB and the yield was 38.5% from [^{11}C]$COCl_2$.[3]

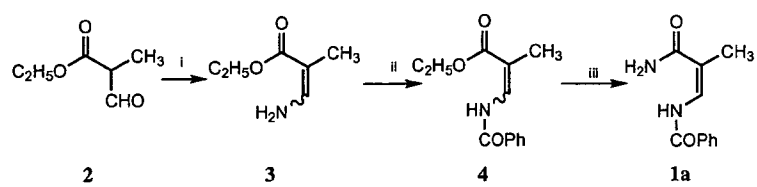

Scheme 2. Synthesis of β-(*N*-benzoylamino)methacrylamide (**1a**). Reagents and conditions: (i) NH_3, CH_3OH, reflux, 2 h; (ii) PhCOCl, C_5H_5N, $CHCl_3$; (iii) NH_3, CH_3OH.

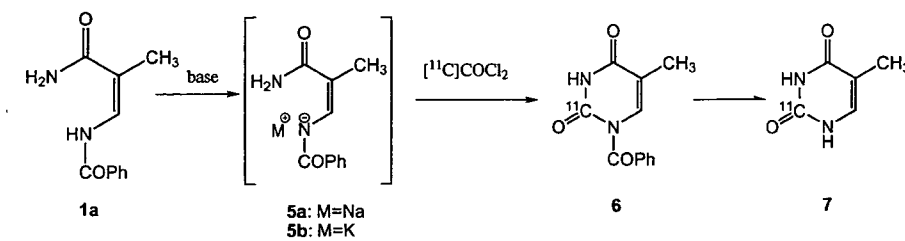

Scheme 3. Synthesis of [2-^{11}C]thymine (**7**).

Table 1. Yields of [2-^{11}C]thymine (7)

Solvent	Base	Mol equiv	Yield (MBq, EOS)
DME	—	—	ND
Toluene	NaH	5	41 ($n = 2$)
DME	NaH	2	68 ± 65 ($n = 3$)
DME	$(CH_3)_3COK$	2	137 ($n = 2$)
DME	$(CH_3)_3COK$	1	362 ± 53 ($n = 3$)

EOS: end of synthesis. ND: not detected. DME: 1,2-dimethoxyethane.

Although previous synthesis of [2-^{11}C]thymine via [^{11}C]urea is more efficient, our strategy involving the cyclocondensation with [^{11}C]$COCl_2$ for the direct production of [2-^{11}C]thymine is operationally simple, and offers fewer reaction steps at lower temperature. The total synthesis described herein takes 16 min from EOB to isolation of **7**, thus significantly shortening the reaction time, which is a crucial consideration for the preparation of short half-life radiopharmaceuticals.

In conclusion, we have provided a substantially useful method for the synthesis of [2-^{11}C]thymine. Having several merits over hitherto known methods, that is fewer reaction steps, mild reaction conditions, reliability of product yield, and simplified operations and synthetic instruments, the present methodology should find wide application in the preparation of many ^{11}C labeled radiopharmaceuticals. Extension of this method to the synthesis of other uracils and nucleosides is currently under investigation in our laboratory.

Acknowledgments

This study was supported in part by Grants-in-Aid for General Scientific Research and 'Academic Frontier' Project from the Ministry of Education, Culture, Sports, Science and Technology of Japan.

References and notes

1. Toyohara, J.; Fujibayashi, Y. *Nucl. Med. Biol.* **2003**, *30*, 681–685, and references cited therein.
2. Vander Borght, T.; Labar, D.; Pauwels, S.; Lambotte, L. *Int. J. Appl. Radiat. Isot.* **1991**, *42*, 103–104.
3. Steel, C. J.; Brady, F.; Luthra, S. K.; Brown, G.; Khan, I.; Poole, K. G.; Sergis, A.; Jones, T.; Price, P. M. *Appl. Radiat. Isot.* **1999**, *51*, 377–388.
4. Link, J. M.; Grierson, J. R.; Krohn, K. A. *J. Label. Compd. Radiopharm.* **1995**, *37*, 610–612.
5. Chakraborty, P. K.; Mangner, T. J.; Chugani, H. T. *Appl. Radiat. Isot.* **1997**, *48*, 619–621.
6. Vander Borght, T.; Pauwels, S.; Lambotte, L.; De Saeger, C.; Beckers, C. *J. Label. Compd. Radiopharm.* **1990**, *28*, 819–822.
7. Nishijima, K.; Kuge, Y.; Seki, K.; Ohkura, K.; Motoki, N.; Nagatsu, K.; Tanaka, A.; Tsukamoto, E.; Tamaki, N. *Nucl. Med. Biol.* **2002**, *29*, 345–350.
8. Nishijima, K.; Kuge, Y.; Seki, K.; Ohkura, K.; Morita, K.; Nakada, K.; Tamaki, N. *Nucl. Med. Commun.* **2004**, *25*, 845–849.
9. Cruickshank, K. A.; Jiricny, J.; Reese, C. B. *Tetrahedron Lett.* **1984**, *25*, 681–684.
10. Marx, J. N.; Craig Argyle, J.; Norman, L. R. *J. Am. Chem. Soc.* **1974**, *96*, 2121–2129.
11. Selected data **1a**: (*Z*)-β-(*N*-Benzoylamino)methacrylamide: mp 182–184 °C (recrystallized from 50% AcOEt–hexane). ^{1}H NMR ($CDCl_3$): δ 1.95 (3 H, d, $J = 1.2$ Hz), 5.40–5.80 (2H, br d, D_2O exchangeable, NH_2), 7.46 (2H, t, $J = 7.2$ Hz), 7.54 (1H, t, $J = 7.2$ Hz), 7.54 (1H, d, $J = 7.5$ Hz), 7.93 (2H, d, $J = 7.2$ Hz), 12.3 (1H, br s, D_2O exchangeable, NH). Anal. Calcd for $C_{11}H_{12}N_2O_2$: C, 64.69; H, 5.92; N, 13.72. Found: C, 64.50; H, 6.05; N, 13.60.
12. The chemical purity of the product isolated by HPLC was 99%. Spectroscopic data (NMR, IR, and MS) of the product were completely superimposable on those of authentic thymine.
13. [^{11}C]$COCl_2$ was bubbled with helium flow into a reaction vial containing a solution of **5b** (0.2 mg) in DME (0.5 mL) in the presence of the base at 30 °C for 1 min. After removal of the solvent, treatment of the residual [2-^{11}C]*N*-benzoylthymine (**6**) with 1.5 M ammonia–methanol for 1 min at room temperature resulted in debenzoylation to yield **7**. The reaction mixture was subjected to reverse-phase HPLC equipped with UV monitor and γ counter (μ-Bondapak C_{18}, 25 cm × 0.39 cm i.d., 3% EtOH–Saline, flow rate 0.5 mL/min at 40 °C). The radioactive peak at 11 min was the desired [2-^{11}C]thymine. The product was observed to be 99% radiochemically pure by HPLC.
14. The yield of [2-^{11}C]thymine was determined based on produced [^{11}C]$COCl_2$. We estimated the yield of [^{11}C]$COCl_2$ to be about 1500 MBq based on the yield of diphenylurea.
15. Friedkin, M.; Roberts, D. *J. Biol. Chem.* **1954**, *207*, 257–266.

Development of a novel fluorescent imaging probe for tumor hypoxia by use of a fusion protein with oxygen-dependent degradation domain of HIF-1α

Shotaro Tanaka[a, b], Shinae Kizaka-Kondoh*[a, b, c], Hiroshi Harada[a], & Masahiro Hiraoka[a, b]
[a] Department of Radiation Oncology and Image-applied Therapy, Kyoto University Graduate School of Medicine. 54 Kawahara-cho, Shogoin, Sakyo-ku, Kyoto, 606-8507 Japan. Phone/FAX: +81-75-751-4242; [b] Kyoto City, Collaboration of Regional Entities for the Advancement of Technological Excellence, Japan Science and Technology Agency. Creation Core Kyoto Mikuruma、448-5 Kajiicho, Kamigyo-ku, Kyoto Japan; [c] COE Formation for Genomic Analysis of Disease Model Animals with Multiple Genetic Alterations, Kyoto University Graduate School of Medicine. 54 Kawahara-cho, Shogoin, Sakyo-ku, Kyoto, Japan.

ABSTRACT

More malignant tumors contain more hypoxic regions. In hypoxic tumor cells, expression of a series of hypoxia-responsive genes related to malignant phenotype such as angiogenesis and metastasis are induced. Hypoxia-inducible factor-1 (HIF-1) is a master transcriptional activator of such genes, and thus imaging of hypoxic tumor cells where HIF-1 is active, is important in cancer therapy. We have been developing PTD-ODD fusion proteins, which contain protein transduction domain (PTD) and the VHL-mediated protein destruction motif in oxygen-dependent degradation (ODD) domain of HIF-1 alpha subunit (HIF-1α). Thus PTD-ODD fusion proteins can be delivered to any tissue *in vivo* through PTD function and specifically stabilized in hypoxic cells through ODD function. To investigate if PTD-ODD fusion protein can be applied to construct hypoxia-specific imaging probes, we first constructed a fluorescent probe because optical imaging enable us to evaluate a probe easily, quickly and economically in a small animal. We first construct a model fusion porein PTD-ODD-EGFP-Cy5.5 named POEC, which is PTD-ODD protein fused with EGFP for in vitro imaging and stabilization of fusion protein, and conjugated with a near-infrared dye Cy5.5. This probe is designed to be degraded in normoxic cells through the function of ODD domain and followed by quick clearance of free fluorescent dye. On the other hand, this prove is stabilized in hypoxic tumor cells and thus the dye is stayed in the cells. Between normoxic and hypoxic conditions, the difference in the clearance rate of the dye will reveals suited contrast for tumor-hypoxia imaging. The optical imaging probe has not been optimized yet but the results presented here exhibit a potential of PTD-ODD fusion protein as a hypoxia-specific imaging probe.

Keywords: Tumor hypoxia, Near-infrared (NIR) fluorescent imaging, Oxygen-dependent degradation (ODD), Hypoxia-inducible Factor (HIF)-1α, Protein Transduction Domain (PTD)

1. INTRODUCTION

Solid tumors often contain hypoxic regions with reduced oxygen tension far below physiological levels (1). Detecting hypoxic regions in tumor is very important for cancer therapies because of the following reasons; 1) Hypoxic regions are formed as a consequence of rapid tumor growth and profoundly disorganized vasculature (1-3); 2) Hypoxic tumor cells are resistant to radiotherapy and chemotherapy (2); 3) In hypoxic tumor cells, hypoxia-inducible transcriptional factors, such as HIF-1, induce various hypoxia-responsive genes, which confer malignant phenotypes of tumors such as apoptosis resistance, tumor growth, invasion and metastasis (2-4) and thus HIF-1 expression is closely associated with malignancy and poor prognosis; 4) Hypoxic region is detected in experimental tumors less than 1 mm in diameter.

Genetically Engineered and Optical Probes for Biomedical Applications IV, Samuel Achilefu, Darryl J. Bornhop, Ramesh Raghavachari, Alexander P. Savitsky, Rebekka M. Wachter, Eds., Proc. of SPIE Vol. 6449, 64490Y, (2007) · 1605-7422/07/$18 · doi: 10.1117/12.713633

HIF-1 is the major hypoxia-inducible transcription factor composed of α and β subunits (4-6). HIF-1α is regulated in an oxygen-dependent manner at the post-translational level (4, 5), while HIF-1β is constitutively expressed. HIF-1α contains oxygen-dependent degradation (ODD) domains (4, 5, 7) and is hydroxylated at proline residues in ODD domain by 4-prolyl hydroxylases (PHDs) (8, 9). The modification accelerates the interaction of the HIF-1α protein with the von Hippel-Lindau (VHL) tumor suppressor protein (10, 11), resulting in the rapid ubiquitination and subsequent degradation of the protein by the 26S proteasome (8-12). Thus oxygen-dependent regulation of HIF-1 activity is absolutely dependent on the stability of HIF-1α protein.

We have developed fusion proteins containing $ODD_{548-603}$, which has VHL-mediated protein destruction motif of HIF-1α and demonstrated that stability of the ODD fusion proteins are regulated by oxygen concentration as the same manner as HIF-1α (13). That is, the fusion proteins are rapidly degraded in normoxic cells and stabilized in hypoxic cells. Furthermore, we fused a protein transduction domain (PTD) to ODD fusion protein and demonstrated that resultant PTD-ODD fusion proteins are still under the same oxygen-dependent regulation as HIF-1α (13) and delivered to hypoxic cells in tumors (14-18).

Here we report a PTD3-ODD fusion protein as a novel probe for imaging hypoxic regions in tumors. PTD3 is a novel amphipathic one, which consists of poly-cathionic domain and hydrophobic domain. To evaluate the efficacy of PTD-ODD fusion protein as a hypoxia-specific probe, we conjugated a near infrared fluorescent (NIRF) dye Cy5.5 and examined bio-kinetics of the probe in tumor-bearing mice.

2. METHODOLOGY

2.1 Plasmid construction

The plasmids for preparing recombinant proteins EGFP, PTD3-ODD-EGFP and poly-Lysine (K9)-EGFP were constructed by inserting their encoding sequences to pGEX6P3 vector (GE healthcare Bio-Science Corp. Piscataway, NJ).The coding sequences of EGFP were obtained by PCR amplification with pEGFP vector (Chlontech Mountain View, CA) as a template. PTD3 (KKKKKKKKKETWWETWWETW), and K9 (KKKKKKKKK) coding sequences were constructed by annealing corresponding oligonucleotides. The DNA fragment encoding ODD was obtained from pGEX6P3-TAT-ODD-Procaspase-3 plasmid (14) by digesting it with *Bgl*II and *Kpn*I.

2.2 Cell culture and hypoxia-mimic treatment *in vitro*

HeLa/5HRE-Luc cells (17) were maintained at 37°C in 5% FBS-Dulbecco's modified Eagle medium (DMEM, Nacalai Tesque, Kyoto, Japan) supplemented with penicillin (100 units/ml) and streptomycin (100 μg/ml).

For hypoxia-mimic condition, cells were treated with medium and buffers containing $CoCl_2$ (final concentration at 100 μM), which inhibits the oxygen-dependent degradation function of 4-prolyl hydroxylases (8). To observe oxygen-dependent degradation of POEC, HeLa/5HRE-Luc ($1X10^5$) cells were cultured in 35-mm dish, washed twice with saline, and incubated with saline containing POEC (0.72 nM) in 30 min at 37 °C with/without $CoCl_2$. Then the cells were washed with PBS and harvested by trypsinization to analyze Cy5.5-fluorescence intensity by IVIS200™ imaging system (Xenogen Corp., Alameda, CA). Obtained images were analyzed by Living Image 2.50-Igor Pro 4.09A software ((Xenogen Corp., Alameda, CA). Each experiment was repeated four times.

2.3 Preparation of PTD3-ODD-EGFP-Cy5.5

Fusion protein PTD3-ODD-EGFP (POE), K9-EGFP and EGFP was prepared by the basically same method as described previously (14) and dissolved at the final concentration of 1.0 mg/ml in PBS (pH 8.0). The NIRF dye, Cy5.5-NHS (GE healthcare Bio-Science Corp.), was reacted with POE fusion protein for 1 hr at room temperature. Then the reacted solution was treated by desalting column (Sephadex G-50, GE healthcare Bio-Science Corp.) equilibrated PBS (pH 8.0) to remove non-labeled free dye. The eluting fraction of Cy5.5-labelled POE (PTD3-ODD-EGFP-Cy5.5; POEC) was concentrated to the final concentration of 1.0 mg/ml by ultrafiltration (Amicon Ultra 10k, Millipore, Bollerica, MA). The absorbance of 280 and 675 nm were measured, and efficiency of labeling was determined by following the manufacturer's instruction manual.

2.4 Trypsin-digestion and SDS-PAGE analysis

Trypsin-digestion of and SDS-PAGE were undertaken to identify Cy5.5-labeled region of POEC. Trypsine (2.5 mg/ml) 5 μl was added into 100 μl of POEC solution (1.0 mg/ml) and incubation in 30 min at room temperature. Finally, 5 μl of the product was applied on SDS-PAGE (15% aclylamide gel). After electrophoresis, the gel was analyzed by using IVIS200™ imaging system for Cy5.5 fluorescence detection (Fig. 2A). The maximum excitation- and emission wavelength of POEC was measured by using fluorescent spectrometer RF-5300PC (SHIMADZU, Kyoto, Japan).

2.5 Assessment of membrane transduction activity by flow cytometric analysis

To evaluate the membrane transduction activity of the fusion proteins with various protein transduction domains, HeLa/5HRE-Luc cells (1 x 10^5/well) were seeded in a 24-well plate. The following day, the cells were washed 3 times with PBS (pH 7.5) and cultured in 200 μl of serum-free DMEM with a fusion protein (approximately 50 μg). The amount of fusion protein was adjusted based on the EGFP fluorescent intensity. After 30 min incubation in CO_2 incubator, the cells were washed 3 times with DMEM (without FBS), once with PBS containing 0.02% EDTA, and then treated with 200 μl of 0.25% trypsin-EDTA solution at 37 °C for 5 min, and added 1ml of 5%FBS-DMEM. The cells were harvested and washed with PBS (pH 7.5) at once. Finally, the cells were re-suspended in 300 μl of ice-cold PBS (pH 7.5) and kept on ice. In case of the experiments for ODD-fusion protein, the cells were treated with the reagents containing $CoCl_2$ (final concentration at 100 μM) to inhibit oxygen-dependent degradation of ODD-fusion proteins. The EGFP fluorescent intensity of the cells was determined by flow cytometric analysis using CELLQuest (Becton-Dickinson, Mountain View, CA).

2.6 Xenograftic tumor formation

Cell suspensions of HeLa/5HRE-Luc cells (1 x 10^6 cells / 100 μl of PBS) were inoculated subcutaneously in the left and right hind legs of 8-week-old male nude mice (BALB/c *nu/nu*; Japan SLC, Hamamatsu, Japan). The mice were used for experiments 2 weeks after implantation.

2.7 In vivo fluorescence and luciferase imaging

The tumor bearing mice were intravenously injected with fluorescent dye-labeled probes and certain time after injection they were applied to IVIS200™ system. This system collects photons of light emitted from mice through corresponding fluorescence filters using the cooled charge-coupled device camera.

To detect bioluminescence from xenografts of HeLa/5HRE-Luc cells (17), tumor-bearing mice were intraperitoneally injected with 100 μl D-luciferin solution (10 mg/ml in PBS; Promega Corp., Madison, WI). Ten minutes later the mice were put in IVIS200™ ((Xenogen Corp., Alameda, CA). During the imaging, the mice were kept under anesthesia with 2.5% of isoflurane gas in oxygen flow (1.5 L/min). Obtained images were analyzed by Living Image 2.50-Igor Pro 4.09A software ((Xenogen Corp., Alameda, CA).

3. RESULTS

3.1 Design of hypoxia-specific probe PTD3-ODD-EGFP-Cy5.5 (POEC)

To image hypoxic tumor cells *in vivo*, we constructed a model fusion protein PTD3-ODD-EGFP-Cy5.5 (POEC), which consists of four functional parts, PTD3, ODD, EGFP, and Cy5.5 (Fig. 1A). PTD3 is a novel amphipathic PTD which was constructed with poly-cathionic domain and hydrophobic domain. PTD3 was fused on POEC to delivery the probe into cytosol of whole cells in the body through cell membrane. ODD is a part of ODD domain (548-603) of HIF-1α (ref), which is the VHL-mediated protein destruction motif of HIF-1α so that they can be degraded rapidly in normoxic cells and stabilized in hypoxic cells (13). Enhanced green fluorescent protein (EGFP) functions as a carrier and an in vitro imaging. Cy5.5 is for *in vivo* imaging, whose fluorescence wavelengths (650-700 nm) are suit for *in vivo* imaging because of its high transmittance, low interference and non-invasive on tissue. POEC is designed as follows: In normoxia, Cy5.5 is released from POEC at the protein degradation and goes out directly of cells because of its small

molecular weight: In hypoxic cells, Cy5.5 is remained in the cells because POEC is stabilized. These differences of the Cy5.5 clearance speed between normoxic and hypoxic cells would make marked contrast, resulting in visualization of tumor hypoxia.

3.2 Evaluation of POEC in vitro

The labeling-efficiency of the prepared POEC with Cy5.5 was 1.38, which was calculated by using the values of absorbance with 280 nm and 678 nm. The excitation- and emission wavelength of POEC were 683.4 nm and 697.0 nm, respectively, which are slightly different from Cy5.5-NHS (675 nm and 694 nm). The Labeled PTD3-ODD-EGFP (POE) retained EGFP fluorescence. The result of gel filtration revealed that the probe was monomer at that condition (data not shown).

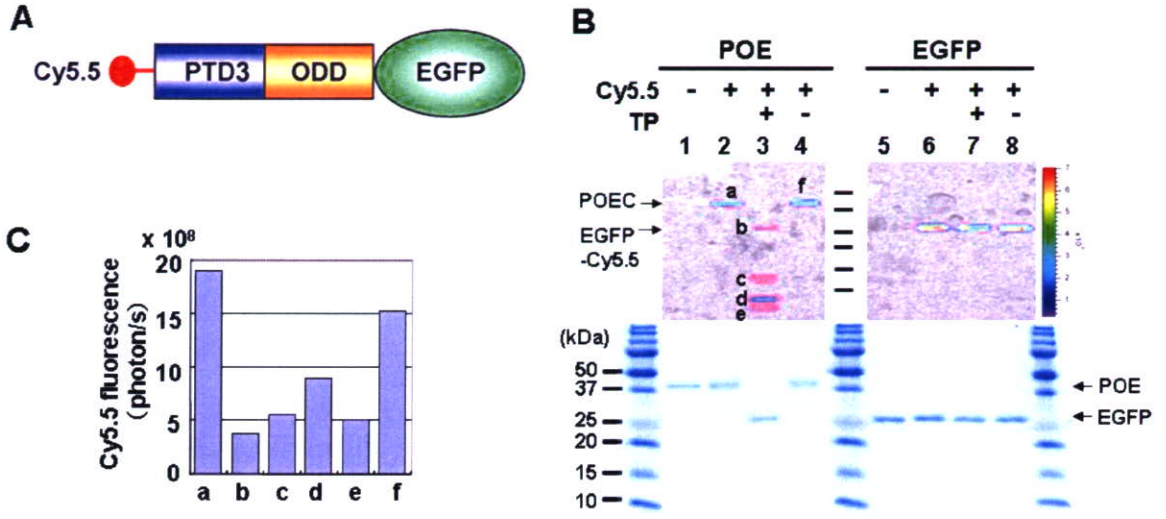

Fig. 1. Structural analysis of PTD3-ODD-EGFP-Cy5.5 (POEC). A. Diagram of POEC. **B.** Analysis of Cy5.5-labeling site. Purified PTD3-ODD-EGFP (left) and EGFP (right) were labeled with Cy5.5 (+; lanes 2-4 and 6-8 respectively) and digested with trypsin (TP +; lane 3 and 7 respectively), or untreated (lane 1 and 5, respectively). After electrophoresis, Cy5.5 fluorescent signal of the SDS-PAGE gel (15%) were detected by using IVIS200™ imaging system (upper panel) and then the gel was stained by CBB (lower panel). **C.** Cy5.5 fluorescent intensity. Fluorescence intensity of the Cy5.5-labeled polypeptides (a-f) in Figure 1B is shown in the graph.

3.2.1 Cy5.5-labeled domain

POEC was digested by trypsin to identify Cy5.5-labeled site. Trypsinized POEC was separated into four fragments: three smaller fragments (approximate molecular weight 5, 7 and 13 kDa) and the largest fragment with the same size as EGFP (approximate molecular weight: 27 kDa) (Fig. 1B, lower panel, lane 3). EGFP fluorescence intensity of the trypsinized POEC was similar to the one of undigested one (data not shown), indicating that EGFP domain was not digested by trypsin and that three smaller fragments were came from PTD-ODD domain. Cy5.5 fluorescence intensity analysis of SDS-PAGE gel demonstrated that while Cy5.5 fluorescence was observed on all the digested POEC fragments, about 83.7% of the total fluorescent intensity (the sum of b-e) was detected in PTD3-ODD region (fragment c-e) (Fig. 2B lower panel lane 3 and 2C). These results indicate that Cy5.5 was mainly located in PTD3-ODD domain. Because no lysine residue exists in the ODD domain and the labeling efficiency was nearly 1.0, Cy5.5 may mainly locate at N-terminal of PTD3 domain.

3.2.2 Membrane transduction activity

PTD function contributes *in vivo* delivery of PTD-fusion proteins (ref). Thus we evaluated membrane transduction activity of PTD3 after fused with ODD-EGFP and further labeled with Cy5.5. The membrane transduction activity of PTD-fusion proteins was examined by EGFP fluorescent intensity of the cells treated with PTD-fusion proteins: When higher membrane transduction activity PTD-fusion protein has, more EGFP fluorescent intensity the cells treated with it has. The cells treated with EGFP without PTD domain showed the same fluorescent intensity as untreated cells (data not shown). The cells treated with POE showed the similar fluorescent intensity to the ones treated with K9-EGFP, indicating that PTD3 has compatible membrane transduction activity as poly-Lysine (Fig. 2A).

Next we examined the influence of Cy5.5-labeling on the membrane transduction activity of PTD3 because the Cy5.5-labeling domain analysis indicated that Cy5.5-labeling site was mainly in PTD3 domain (Fig. 1A and 1B). The membrane transduction activity of POEC was slightly decreased compared to unlabelled POE (Fig. 2B), suggesting modification of PTD domain influence the PTD function. Although labeling with Cy5.5 slightly diminished the PTD ability of POE (Fig. 3B), the membrane transduction activity of PTD3 in POEC was still high.

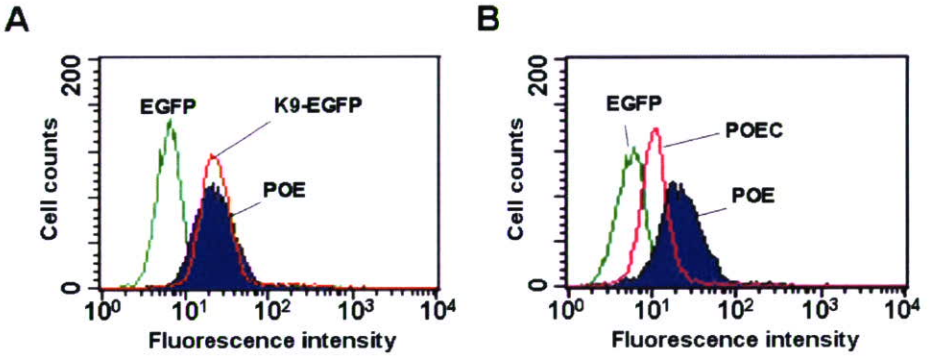

Fig. 2. FACS analysis of membrane transduction activity of PTD-fusion protein. EGFP or PTD-fusion proteins were added into the culture medium (serum-free DMEM) of HeLa/5HRE-Luc cells. After 30 min incubation in 37 °C, the cells were washed by PBS, trypsinized, and harvested and EGFP fluorescent intensity was analyzed with FACS. Each experiment was done in triplicate and repeated at least twice. **A.** EGFP, poly-Lysine (K9)-EGFP and POE were treated as described above and their EGFP fluorescent intensities are shown in graph. **B.** EGFP, POE and POEC were treated as described above and their EGFP fluorescent intensities are shown in graph.

3.2.3 Oxygen-dependent degradation of POEC *in vitro*.

Oxygen-dependent degradation regulation of POEC was examined by IVIS200™ imaging system. The cells were incubated with medium containing POEC with or without $CoCl_2$ and then Cy5.5 fluorescence intensity was examined with IVIS200™ imaging system (Fig. 3). Since the amount of stabilized POEC protein was very small, EGFP fluorescence of POEC was not detectable. On the other hand, the Cy5.5 fluorescence was sensitive enough to detect POEC (Fig. 3 right) because of their higher fluorescence intensity and longer residence time compared with EGFP. Under the same observation conditions, however, significantly less Cy5.5 fluorescence was observed in the cells treated without $CoCl_2$ (Fig.3 middle). Similar results were obtained by the experiment with other hypoxia-mimic reagent, FDG, which inhibits PHD2 by chelating Fe ions. These data demonstrate that the stability of POEC protein is regulated by PHD, thus oxygen concentration. No fluorescence was detected in any cells by the same experiment using Cy5.5-glycine (data not shown), suggesting small polypeptides labeled with Cy5.5 may easily go out of the cells.

3.3 Bio-kinetics of POEC in tumor-bearing mice

We have already reported that PTD-ODD-β-galactosidase fusion protein was delivered and stabilized in hypoxic regions in tumors after intraperitoneal injection of the fusion protein (14). In present study, we examined if POEC could function as an optical probe specific to tumor hypoxia. Because HeLa/5HRE-Luc cells stably retain a luciferase reporter gene under the control of HIF-1-responsive promoter (17), the existence of hypoxic regions in tumor xenografts was visualized by imaging of hypoxia-responsible expression of luciferase in the tumors (Fig. 4). Cy5.5 fluorescence image was detected in entire bodies within a few minutes after administration of POEC, then the image became thinner and 24 hr after the probe administration, the fluorescent image in the tumors became high contrast compared with their surrounding regions, and reached high magnitude of fluorescence (Fig. 4, upper panels, red cycles). High accumulation of Cy5.5 fluorescence was observed in some specific organs such as kidney, liver, bladder and small intestine. Strong fluorescent signals were observed in the entire area of the back. Although strong fluorescent signal was also observed in the back of non-tumor bearing mice, no fluorescent signal was observed in their hind legs 24 hr after the probe administration (Fig. 4, middle panels). When Cy5.5-EGFP was injected into tumor bearing mice, although some images were also detected in tumors (Fig. 4, lower panels, blue cycles), the image were much smaller and stay shorter than the one of POEC image. The non-specific fluorescent signals of Cy5.5-EGFP in the back were also weaker than that of POEC. The fluorescent signals in the tumors and the back of the mice gradually decreased day by day, but remained until 1 to 2 weeks in detectable magnitude. Now we are examining POE labeling with other NIR dye and obtaining more tumor specific images (much lower background). We are going to confirm the specificity of the probes to hypoxic tumor cells by immuno-histochemical analysis.

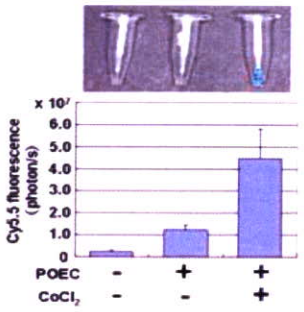

Fig. 3. Analysis of ODD regulation of POEC. The cells were treated with (+) or without (-) POEC as Figure 2 legend. For the hypoxia-mimic treatment, the medium and reagents contained PHD inhibitor ($CoCl_2$). The cells were harvested and analyzed for Cy5.5-fluorescenct intensity by using IVIS200™ imaging system. The experiment was done in triplicate. The representative images are shown in upper panel and average fluorescence intensity of each sample is shown in lower graph.

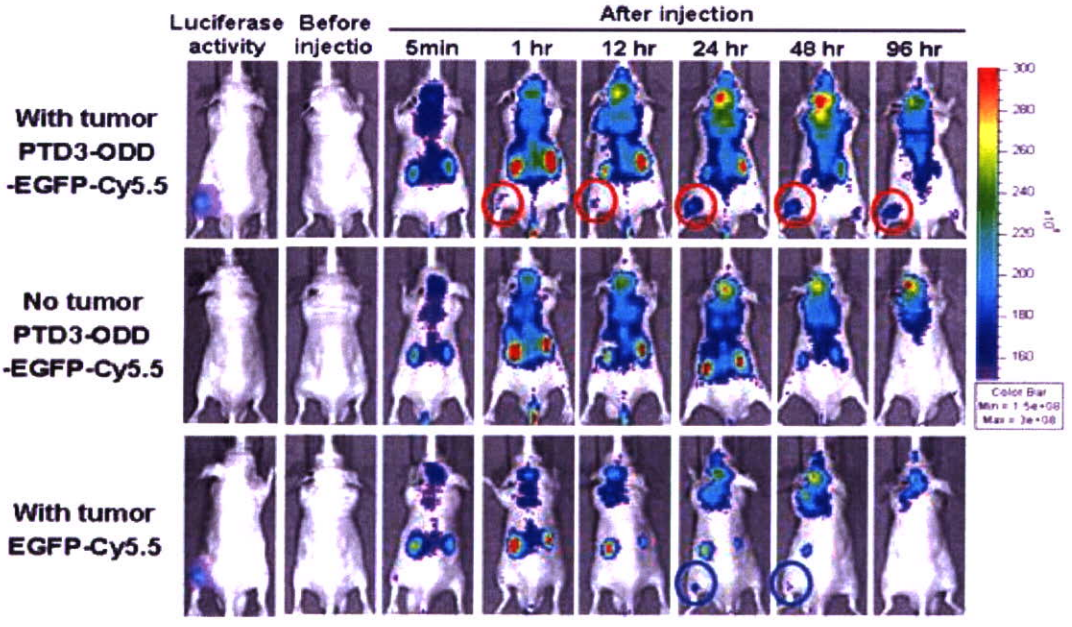

Fig. 4. In vivo fluorescence imaging of POEC. POEC and EGFP-Cy5.5 (1.0 nmol per body) were intravenously injected to tumor-free or tumor-bearing nude mice. Cy5.5 fluorescent signal was detected by IVIS200™ imaging system at the indicated time after probe injection. Image in tumor of POEC (red cycle) and EGFP-Cy5.5 (blue cycle) are shown in figure.

4. CONCLUSION

In this study, we reveal that a PTD-ODD fusion protein has potential to make a unique probe for detecting tumor hypoxia. Because tumor hypoxia is a hallmark of malignancy and poor prognosis, such a probe would open a new avenue in both cancer diagnosis and therapies. At the same time, we can demonstrate that an optical imaging system is a very useful tool to evaluate the specificity of a probe *in vivo*. In our evaluation system, we made the best use of the multiplicity of optical imaging: we visualized the target of tumor hypoxia by bioluminescence imaging using a luciferase reporter vector containing a hypoxia-responsive promoter, and evaluate bio-kinetics of the probe with fluorescence imaging. Such optical imaging systems can accelerate the development of new probes for therapeutic and diagnostic use.

ACKNOWLEDGEMENT

We would like to thank Dr. Kazuhiro Tanabe (Department of Energy and Hydrocarbon Chemistry, Faculty of Engineering, Kyoto university, Kyoto, Japan) for fluorescent spectrometer technical support; Ms. Yumi Takahashi, Akiyo Morinibu and Kazumi Shinomiya for assistance. This study is a part of Kyoto City Collaboration of Regional Entities for the Advancement of Technological Excellence of JST on basis of research results supported in part by grant-in aids for Scientific Researches (A) (No.14205037 and No.15201033).

REFERENCES

1. P. Vaupel, F. Kallinowski and P. Okunieff, "Blood flow, oxygen and nutrient supply, and metabolic microenvironmento of human tumors: a review", Cancer Res. 49 (23), 6449-6465 (1989).
2. Brown JM, Wilson WR. Exploiting tumour hypoxia in cancer treatment. Nat Rev Cancer. 2004 Jun;4(6):437-47.
3. Harris AL. Hypoxia--a key regulatory factor in tumour growth. Nat Rev Cancer. 2002 Jan;2(1):38-47.
4. G. L. Semenza, "Regulation of mammalian O_2 homeostasis by hypoxia-inducible factor 1", Annu. Rev. Cell. Dev. Biol.15, 551-578 (1999).
5. G. L. Semenza, "Targeting HIF-1 for cancer therapy", Nat. Rev. Cancer (3), 721-732 (2003).
6. G. L. Semenza and G. L. Wang, "A nuclear factor induced by hypoxia via de novo protein synthesis binds to the human erythropoietin gene enhancer at a site required for transcriptional activation", Mol. Cell. Biol. 12, 5447-5454 (1992).
7. L. E. Huang, J Gu, M. Schau and H. F. Bunn, "Regulation of hypoxia-inducible factor 1 alpha is mediated by an O2-dependent degradation domain via the ubiquitin-proteasome pathway", Proc. Natl. Acad. Sci. U S A 95, 7987-7992 (1998).
8. R. K. Bruick and S. L. McKnight, "A conserved family of prolyl-4-hydroxylases that modify HIF", Science 294, 1337-1340 (2001).
9. A. C. Epstein, J. M. Gleadle, L. A. McNeill LA, et al., "C. elegans EGL-9 and mammalian homologs define a family of dioxygenases that regulate HIF by prolyl hydroxylation", Cell 107, 43-54 (2001).
10. M. E. Cockman, N. Masson, D. R. Mole, et al., "Hypoxia inducible factor-alpha binding and ubiquitylation by the von Hippel-Lindau tumor suppressor protein", J. Biol. Chem. 275, 25733-25741 (2000).
11. M. Ohh, C. W. Park, M. Ivan, et al., "Ubiquitination of hypoxia-inducible factor requires direct binding to the beta-domain of the von Hippel-Lindau protein", Nat. Cell. Biol. 2, 423-7 (2000).
12. P. J. Kallio, W. J. Wilson, S. O'Brien, Y. Makino and L. Poellinger, "Regulation of the hypoxia-inducible transcription factor 1alpha by the ubiquitin-proteasome pathway", J. Bio.l Chem. 274, 6519-6525 (1999).
13. H. Harada, S. Kizaka-Kondoh, M. Hiraoka. "Mechanism of hypoxia-specific cytotoxicity of procaspase-3 fused with a VHL-mediated protein destrauction motif of HIF-1α containing Pro564". FEBS Lett. 580, 5718-5722 (2006)

14. H. Harada, M. Hiraoka, S. Kizaka-Kondoh. "Antitumor effect of TAT-oxygen-dependent degradation-caspase-3 fusion protein specifically stabilized and activated in hypoxic tumor cells". Cancer Res. 62, 2013-2018 (2002).
15. S. Kizaka-Kondoh, M. I noue, H. Harada, M. Hiraoka. "Tumor hypoxia: A target for selective cancer therapy" Cancer Sci. 94, 1021-1028 (2003)
16. M. Inoue, M. Mukai, Y. Hamanaka, M. Tatsuta, M. Hiraoka, S. Kizaka-Kondoh. "Targeting hypoxic cancer cells with a protein prodrug is effective in experimental malignant ascites" Int J Oncol. 25, 713-720 (2004)
17. H. Harada, S. Kizaka-Kondoh, M. Hiraoka. "Optical imaging of tumor hypoxia and evaluation of efficacy of a hypoxia-targeting drug in living animals" Mol Imaging 4, 182-193 (2005).
18. H. Harada, S. Kizaka-Kondoh, M.Hiraoka "Antitumor protein therapy; application of the protein transduction domain to the development of a protein drug for cancer treatment" Breast Cancer 13, 16-26 (2006).

*e-mail: skondoh@kuhp.kyoto-u.ac.jp; phone: +81-75-751-4242; fax: + 81-75-771-9749

FEBS Letters 580 (2006) 5718–5722

Mechanism of hypoxia-specific cytotoxicity of procaspase-3 fused with a VHL-mediated protein destruction motif of HIF-1α containing Pro564

Hiroshi Harada[a,b], Shinae Kizaka-Kondoh[a,c,*], Masahiro Hiraoka[a]

[a] *Department of Radiation Oncology and Image-applied Therapy, Kyoto University Graduate School of Medicine, 54 Kawahara-cho, Shogoin, Sakyo-ku, Kyoto 606-8507, Japan*
[b] *Nano-Medicine Merger Education Unit, Kyoto University, Japan*
[c] *COE Formation for Genomic Analysis of Disease Model Animals with Multiple Genetic Alterations, Kyoto University Graduate School of Medicine, Japan*

Received 29 July 2006; revised 9 September 2006; accepted 11 September 2006

Available online 22 September 2006

Edited by Veli-Pekka Lehto

Abstract Under normoxic conditions the alpha-subunit of hypoxia-inducible factor (HIF-1α) protein is targeted for degradation by the von Hippel-Lindau (VHL) tumor suppressor protein acting as an E3 ubiquitin ligase. Recently, we developed a hypoxia-targeting protein, TOP3, which consisted of procaspase-3 with the VHL-mediated protein destruction motif of HIF-1α. This design enables procaspase-3 to be regulated similarly with HIF-1α, being degraded under normoxia while stabilized under hypoxia. Furthermore, stabilized TOP3 was cleaved by the hypoxic stress-induced endogenous caspases and thus the procaspase-3 was converted to active caspase-3 specifically under hypoxic conditions. These data demonstrated that the VHL-mediated protein destruction motif of HIF-1α endowed procaspase-3 with hypoxia-specific cytotoxicity.

Keywords: Hypoxia-inducible factor-1; von Hippel-Lindau; Caspase-3; Hypoxia; Apoptosis

1. Introduction

Hypoxia-inducible factor (HIF) is a transcriptional complex that mediates a broad range of cellular and systemic responses to hypoxia [1]. HIF-1 is a heterodimer composed of α and β subunits, and α subunit of HIF-1 (HIF-1α) is regulated in an oxygen-dependent manner at the post-translational level [2–4]. HIF-1α contains oxygen-dependent degradation (ODD) domains, which contains proline residues, proline-402 and proline-564. In normoxia, HIF-1α is hydroxylated at these proline residues by prolyl-4-hydroxylases [5,6]. The modification accelerates the interaction of the HIF-1α protein with the von Hippel-Lindau (VHL) tumor suppressor protein, resulting in the rapid ubiquitination and subsequent degradation of the protein by the 26S proteasome [7–10].

Recently, we screened ODD domain mutants of human HIF-1α protein and determined the $ODD_{548-603}$, which endowed fusion proteins with sufficient oxygen-dependent degradation regulation [11]. In order to specifically eradicate HIF-1α-expressing hypoxic cells in solid tumors, we constructed procaspase-3 fused with $ODD_{548-603}$ and HIV-Tat protein-transduction domain (PTD). The final product was named TOP3 (Tat-ODD-Procaspase-3) [11–14]. The HIV-Tat PTD domain is derived from human immunodeficiency virus type-1 Tat protein and efficiently delivers TOP3 to any tissue in vivo. The procaspase-3 comes from human caspase-3 protein [15] and confers cytocidal activity to TOP3. We already reported that TOP3 had anti-tumor activity in xenografts model with various cancer cells [11–14] and induced apoptosis to hypoxic tumor cells in xenografts [14].

In the present study, we clarify the mechanism of TOP3 activation and confirm its hypoxia-specific cytotoxity.

2. Materials and methods

2.1. Cell culture and hypoxic treatment in vitro

CFPAC-1 and MIA PaCa-2 human pancreatic cancer cell lines, HeLa human cervical epithelial adenocarcinoma cell line, A549 human lung adenocarcinoma cell line, WiDr human colorectal adenocarcinoma cell line and 786-O human renal cell carcinoma cell line were purchased from the American Type Culture Collection. HeLa/EF-Luc and HeLa/5HRE-Luc cell clones were isolated as described previously [14]. WT8, a 786-O cell clone stably transfected with a plasmid coding hemagglutinin (HA)-tagged VHL, was a kind gift from Dr. William G. Kaelin Jr. [16]. CFPAC-1 was maintained as described previously [11], and the other cells were maintained at 37 °C in 5% FBS-Dulbecco's modified Eagle's medium (Nacalai Tesque, Kyoto, Japan) supplemented with penicillin (100 units/ml) and streptomycin (100 μg/ml).

Hypoxic condition of <0.02% of oxygen tension was attained by the use of a Bactron Anaerobic Chamber, BACLITE-1 (Sheldon Manufacturing Inc., Cornelius, OR). Cells were incubated in the chamber for at least 6 h before various treatments.

2.2. Formulation of TOP3 fusion protein

The Tat-ODD-Procaspase-3 fusion protein (TOP3) was prepared and dissolved in 10 mM Tris–HCl buffer (pH 8.0), as described previously [11]. The final concentration of TOP3 preparation was 15 μg/ml for in vitro experiments if not indicated, and 10 mM Tris–HCl (pH 8.0) was used as the buffer in both in vivo and in vitro experiments if not indicated.

2.3. Experimental procedures for analyses of TOP3 activation in vitro

Cells were pre-incubated under aerobic or hypoxic condition for 6 h, added with TOP3, and incubated further for 20 h before analyses.

As for the Western blot analysis, cells were seeded at 1×10^5 cells/well in a 6-well plate, treated as above and the lysates were prepared by suspending cells from each well in 100 μl of 1 × loading buffer. Twenty μl of the lysate was electrophoresed per lane on a 15% (for

*Corresponding author. Fax: +81 75 771 9749.
E-mail address: skondoh@kuhp.kyoto-u.ac.jp (S. Kizaka-Kondoh).

0014-5793/S32.00
doi:10.1016/j.febslet.2006.09.025

TOP3/caspase-3), a 10% (for VHL) or a 7.5% (for HIF-1α) SDS-polyacrylamide gel. TOP3/caspase-3, VHL and HIF-1α were detected by polyclonal anti-caspase-3 antibody (Cell Signaling Technology Inc., Osaka, Japan), monoclonal anti-HA antibody (Roche Diagnostics Japan, Tokyo, Japan) and monoclonal anti-HIF-1α antibody (BD Bioscience Pharmingen, San Diego, CA), respectively. The polyclonal and the monoclonal primary antibodies were then reacted with anti-rabbit and anti-mouse IgG horseradish peroxidase linked antibodies (Amersham Biosciences Corp., Piscataway, NJ), respectively. Detection was carried out with a chemiluminescence-based method using the ECL-PLUS system (Amersham Biosciences Corp.).

As for the DNA fragmentation analysis, genomic DNA was isolated from 6×10^5 cells with Quick Apoptotic Ladder Detection Kit (BioVision Research Products, Mountain View, CA). DNA was electrophoresed in a 1.5% agarose gel.

As for the FACS analysis, the cells were harvested, gently suspended in PBS and mixed with equal volume of 2 × hypotonic fluorochrome solution (100 μg/ml propidium iodide in 0.2% sodium citrate–0.2% Triton X-100) immediately before the analysis with a flow cytometry using CELLQuest (BD Biosciences, Franklin Lakes, NJ).

As for the analysis of caspase-3 after TOP-3 treatment, the cells were seeded at 2×10^4 cells/well in a 24-well plate, pre-incubated for 16 h and treated with TOP3 for 0, 2, 4, 6 or 8 h. As for the analysis of endogenous capsase-3 and -9 activities, similarly seeded cells were cultured with the medium, which was pre-exposed to hypoxic conditions. Then the cells were incubated under hypoxic or aerobic conditions and harvested after indicated time of incubation. Caspase-3 and -9 activities in 50 μl lysates were measured by using Colorimetric Protease Assay Kit according to the manufacturer's instructions (MBL, Nagoya, Japan). The experiments were done in triplicate and the mean of $OD_{405\,nm}$/50 μg was calculated.

3. Results

3.1. Hypoxia-dependent activation of TOP3

We previously showed citocidal effect of TOP3 on hypoxic cells in the xenografts of a human pancreatic cancer cell line [11,14]. TOP3 was designed to be degraded in normoxic cells through the function of ODD domain of human HIF-1α protein which is sensitive to the VHL-mediated destruction in normoxia. The design allows the conversion of the procaspase-3 domain to active caspase-3 under hypoxia, executing apoptotic killing of the cells.

These expectations were tested as follows. Firstly, the stability of TOP3 was compared with that of HIF-1α protein under aerobic and hypoxic conditions (Fig. 1A). CFPAC-1 cells were cultured under aerobic (lanes 1 and 2) and hypoxic (lanes 3 and 4) conditions and the protein levels of TOP3 and HIF-1α were tested with (lanes 2 and 4) or without (lanes 1 and 3) addition

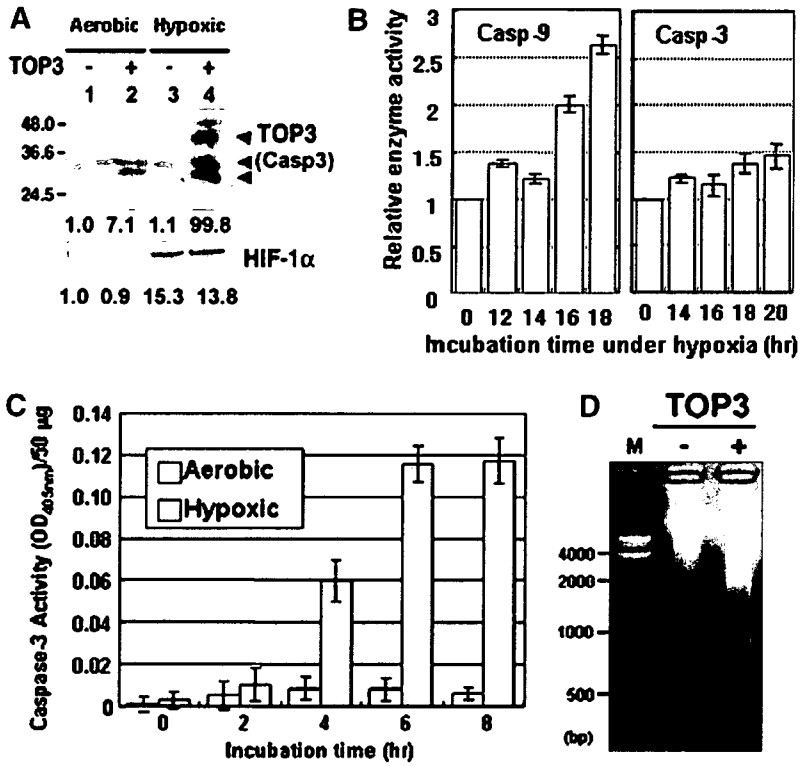

Fig. 1. Hypoxia-dependent stabilization and activation of TOP3 in vitro. (A) CFPAC-1 cells were treated with the buffer only (−; lanes 1 and 3) or TOP3 (+; lanes 2 and 4) under aerobic (lanes 1 and 2) or hypoxic (lanes 3 and 4) conditions for 20 h. TOP3 (upper panel) and HIF-1α (lower panel) proteins in the cells were analyzed by Western blotting with a polyclonal anti-caspase-3 and a monoclonal HIF-1α antibody, respectively. TOP3, its major derivative proteins and endogenous caspase-3 are indicated by arrowheads. The relative density of the bands of TOP3 (upper panel) and HIF-1α (lower panel) proteins of the lanes 2–4 to the lane 1 are indicated below each panel, respectively. (B) CFPAC-1 cells were cultured under hypoxic conditions for indicated period of time and then cell lysates were prepared. Caspase-9 (left) and -3 (right) activities in the cell lysates were measured and relative caspase activities to the 0 h are indicated. (C) CFPAC-1 cells were cultured under aerobic (open bars) and hypoxic (gray bars) conditions for 16 h and then treated with TOP3 or the buffer for the indicated period of time. Total cell lysates were prepared and then $OD_{405\,nm}$ of the lysates was measured. TOP3-derived caspase-3 activity was calculated using the following formula: ($OD_{405\,nm}$/50 μg of the TOP3-treated cells) − ($OD_{405\,nm}$/50 μg of the buffer-treated cells). Results are the means of three independent experiments ± S.D. (D) The cells were treated with the buffer (−) and TOP3 (+) for 20 h under hypoxic conditions. Then the genomic DNA was isolated and analyzed by electrophoresis with a 1.5% agarose gel.

of TOP3. Hypoxic treatment markedly stabilized TOP3 and the protein level was elevated more than 14-fold (Fig. 1A upper panel, lane 2 vs. lane 4). In the same cell preparation, a comparable 14-fold increase was noted for HIF-1α as well (Fig. 1A lower panel, lane 2 vs. lane 4). The control protein without the ODD domain was unaffected by the oxygen tension of the culture (data not shown). These results demonstrate that the stability of TOP3 is sensitive to oxygen concentration as designed.

When CFPAC-1 cells were tested, endogenous caspase-9, the principal caspase in the pathway of mitochondria mediated apoptosis [17], gradually increased and reached the peak after 18 h under hypoxia (Fig. 1B; left panel). However, endogenous caspase-3 activity increased only marginally during the observation period (Fig. 1B; right panel). On the other hand, addition of TOP-3 increased the total caspase-3 activity more than 20-fold when the culture was kept under hypoxia (Fig. 1C). Under this condition, TOP3 induced DNA fragmentation of the cells (Fig. 1D). These results demonstrate that the increase in caspase-3 activity of TOP3-treated cells under hypoxia was due to stabilization and conversion of TOP3 to active caspase-3, resulting in DNA fragmentation. Hypoxia-specific apoptosis induction by TOP3 was also observed other human cancer cell lines such as CFPAC-1, MIA PaCa-2, A549 and WiDr (data not shown), indicating that the function of TOP3 is not cell line-specific.

3.2. VHL-mediated degradation of TOP3

The above observations demonstrate destruction and stabilization of TOP-3 paralleled with those of HIF-1α protein, suggesting that both proteins are under regulation of the VHL mediated degradation system. This was tested by the use of 786-O cells which lacked functional VHL and therefore ubiquitination-mediated degradation through ODD domain does not take place in this cell line. As a positive control, VHL reconstituted WT8 cells were used [16]. In these cells, TOP3 was stabilized if VHL was not expressed (Fig. 2A; upper and lower panels, lane 2) and degraded if VHL was reconstituted (Fig. 2A; upper and lower panels, lane 4). The TOP3 was stabilized (Fig. 2A; upper panel, lanes 6 and 8) and enhanced apoptosis of hypoxic cells (Fig. 2B; lanes 6 and 8) regardless of the VHL status (Fig. 2A; lower panel, lanes 5–8). In contrast, TOP3 did not induce apoptosis regardless of VHL status of the cells as long as the cells were under aerobic conditions (Fig. 2B; lanes 2 and 4).

These results indicate following two. Firstly, the degradation of TOP3 under aerobic conditions is dependent on the VHL function, indicating that it is regulated by the same VHL-mediated protein degradation mechanism as the one of HIF-1α [7–10]. Secondly, the stabilized TOP3 still requires another step to induce apoptosis and this step requires hypoxia.

3.3. Enhancement of hypoxia-induced apoptosis in various cancer cell lines by TOP3

The requirement of hypoxia for the TOP3-induced apoptosis suggests that the cleavage mediated conversion of TOP to caspase-3 is likely to be executed by the endogenous caspases which are activated by hypoxic stress. To assess this possibility, human cancer cell lines, CFPAC-1, MIA PaCa-2, and A549 were treated with TOP3 under hypoxia or normoxia. Morphological observation demonstrated that TOP3 treatment induced cytotoxicity specifically under hypoxia (Fig. 3A). Moreover, FACS analysis confirmed that TOP3 treatment under hypoxic conditions induced degradation of genome DNA as suggested by the increase in the sub-G1 fraction, indicative of the caspase-3 mediated apoptosis of the cells (Fig. 3B). Sub-G1 fraction increased in TOP3 treated CFPAC-1, MIA PaCa-2 and A549 cells under hypoxic conditions by around 10-fold, and were 28.0 ± 2.1%, 27.5 ± 3.8% and 56.5 ± 0.8%, respectively.

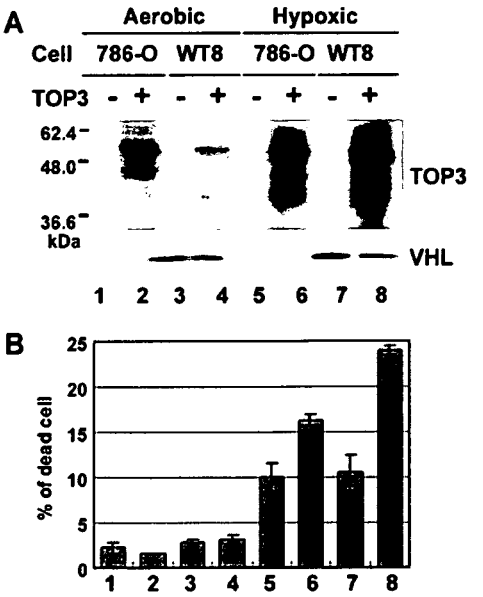

Fig. 2. VHL-dependent ODD regulation of TOP3. 786-O (VHL-deficient renal cell carcinoma cell line) and WT8 (HA-tagged VHL-transfectant clone of 786-O) were treated with the buffer only (−; lanes 1, 3, 5 and 7) or TOP3 (+; lanes 2, 4, 6 and 8) under aerobic (lanes 1–4) or hypoxic (lanes 5–8) conditions. (A) TOP3 (upper panel) and VHL (lower panel) proteins in total cell lysate prepared from each culture were detected by western blot analysis with anti-caspase-3 polyclonal and anti-HA monoclonal antibodies, respectively. (B) DNA contents of these cells were analyzed by flow cytometry and % of population in sub-G1 fraction is indicated as % of dead cell.

4. Discussion

In the present study, we examined the molecular mechanism of activation of procaspase-3 fused with $ODD_{548-603}$, which has VHL-mediated protein destruction motif of HIF-1α containing only 564-proline residue. The results are summarized in Fig. 4.

The ODD domain of HIF-1α including the 564-proline residue physically interacts with VHL which plays a key role in the degradation of the protein through the ubiquitin-proteasome pathway [3–10]. The TOP3 carries the $ODD_{548-603}$ domain and therefore, its ODD regulation was expected to be dependent on VHL expression. Indeed, TOP3 was found to be stable in VHL-deficient 786-O cells even under aerobic conditions (Fig. 2A). These results indicate that TOP3 behaves similarly as HIF-1α and is stabilized in the hypoxic cells in vitro. In our experiments using xenografts, at-ODD-β-galactosidase injected intraperitoneally was specifically detected in the hypoxic regions of tumor xenografts [11]. Present study

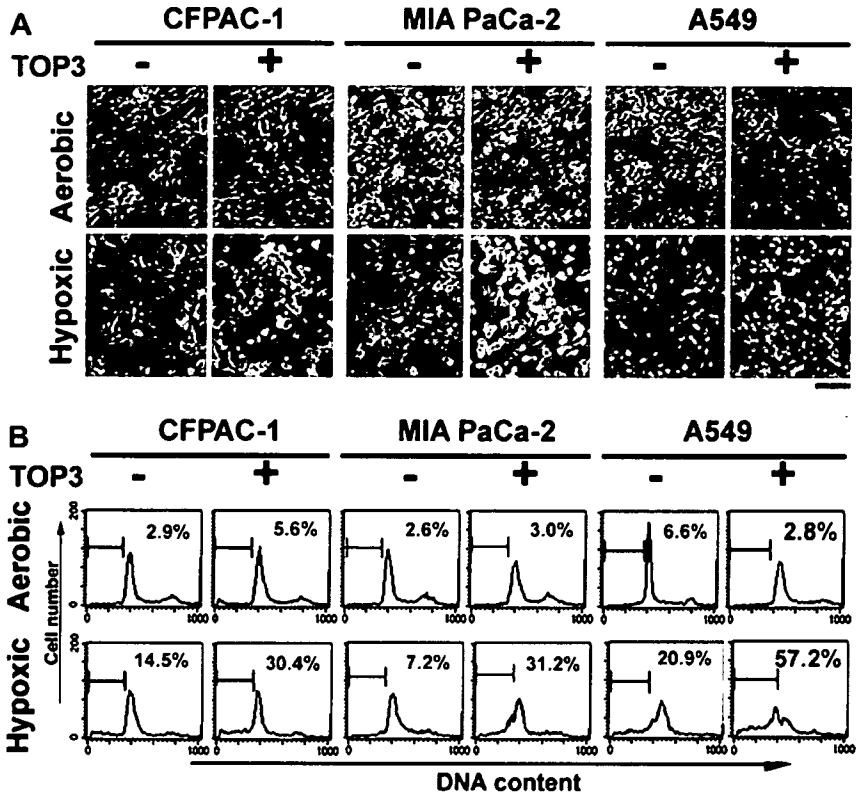

Fig. 3. Enhancement of hypoxia-induced apoptosis by TOP3. CFPAC-1, MIA PaCa-2 and A549 cells were treated with TOP3 (+) or the buffer only (−) for 20 h under aerobic or hypoxic conditions. (A) The morphologies of the cells were observed under an inverted microscope just before FACS analysis. Bar = 200 μm. (B) DNA contents of these cells were analyzed by flow cytometry. % of population in sub-G1 fraction is indicated in each chart. The experiments were done in triplicate and representative photographs (A) and charts (B) are shown.

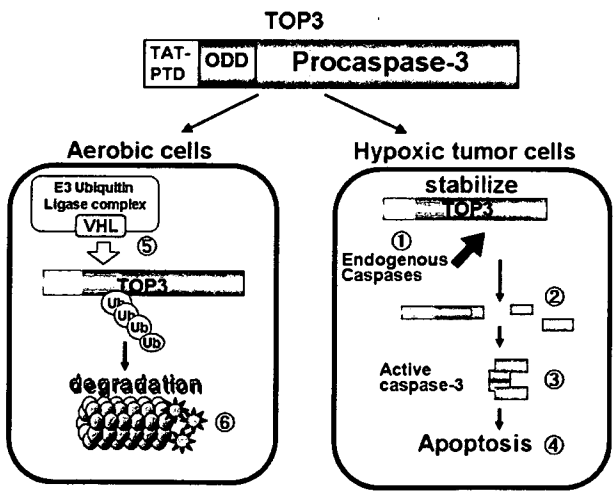

Fig. 4. Mechanism of hypoxia-specific cytotoxicity of TOP3. TOP3 enters in cells by the function of protein transduction domain (PTD) of HIV TAT protein. (1) In hypoxic tumor cells, endogenous caspases are activated to some extent (Fig. 1B). (2) When TOP3 enters in hypoxic tumor cells, TOP3 is cleaved (Fig. 1A, lane 4). (3) Activity of caspase-3 in TOP3-treated hypoxic tumor cells significantly increases (Fig. 1C). (4) DNA fragmentation (Figs. 1D and 3B) is induced and TOP3-treated hypoxic tumor cells undergo apoptosis (Fig. 3). The ODD of TOP3 is the VHL-mediated protein destruction motif of HIF-1α and TOP3 is degraded by VHL-mediated system under normoxia (Fig. 2). (5) When TOP3 enters in aerobic cells, TOP3 is recognized by VHL and (6) degraded through ubiquitin-proteasome system.

confirms that PTD-ODD fusion proteins can be regulated similarly as HIF-1α via VHL-mediated protein destruction motif of HIF-1α in vitro.

Because TOP3 is composed of a dormant form of caspase-3, it has to be cleaved to become active form. That is, stabilization of TOP3 itself cannot induce apoptosis. Indeed, TOP3 was stabilized in 786-O cells under normoxia but did not induce cell death (Fig. 2C). The endogenous caspase activities are brought about by a hypoxic stress (Fig. 1B). Although the major apoptosis pathway induced by hypoxic stress is the mitochondria-mediated 'intrinsic' pathway, in which caspase-9 plays a major role, recent studies suggest the involvement of both the intrinsic and the death receptor-mediated 'extrinsic' pathways in hypoxia-induced apoptosis [18]. TOP3 efficiently enhance the preexisting apoptotic signal leading to more than 20-fold increases of caspase-3 activity (Fig. 1C) and induced DNA fragmentation (Fig. 1D) and cell death (Figs. 2 and 3). All of these characteristics must have contributed not only to the specific targeting of HIF-1α-expressing/hypoxic tumor cells but also to minimizing the obvious side effect to normal tissues in our in vivo experiments [11–14].

It has been reported that hypoxia-induced apoptosis depends on wild-type p53 to a large extent [19–22] and that increased p53 induces apoptosis through a pathway including Apaf-1 and caspase-9 [23]. Thus the extent of hypoxia-induced apoptosis might differ due to p53 status. Interestingly, under hypoxic conditions A549 cells, which possess wild type p53 [24], underwent apoptosis to a larger extent than CFPAC-1

and MIA PaCa-2 cells, which possess mutant type p53 ([25] and Fig. 3).

Acknowledgments: We are grateful to Dr. William G. Kaelin Jr. for 786-O cells and their VHL-expressing clones (WT8); Akiyo Morinibu, Emi Nishimoto, Naoko Murakami-Harada, Yumi Takahashi and Kazumi Shinomiya for skilled technical assistance. This work was supported in part by Grant-in-Aid for Scientific Research on Priority Areas, Cancer, from the Ministry of Education, Culture, Sports, Science and Technology, and by a Grant-in-Aid for the 2nd and 3rd Term Comprehensive 10-Year Strategy for Cancer Control from the Ministry of Health, Labor and Welfare, Japan. This study is a part of joint research, which is focusing on the development of the basis of technology for establishing COE for nano-medicine, carried out through Kyoto City Collaboration of Regional Entities for Advancing Technology Excellence (CREATE) assigned by Japan Science and Technology Agency (JST).

References

[1] Semenza, G.L. (1999) Regulation of mammalian O2 homeostasis by hypoxia-inducible factor 1. Annu. Rev. Cell Dev. Biol. 15, 551–578.
[2] Semenza, G.L. and Wang, G.L. (1992) A nuclear factor induced by hypoxia via de novo protein synthesis binds to the human erythropoietin gene enhancer at a site required for transcriptional activation. Mol. Cell. Biol. 12, 5447–5454.
[3] Huang, L.E., Gu, J., Schau, M. and Bunn, H.F. (1998) Regulation of hypoxia-inducible factor 1 alpha is mediated by an O2-dependent degradation domain via the ubiquitin-proteasome pathway. Proc. Natl. Acad. Sci. USA 5, 7987–7992.
[4] Kallio, P.J., Wilson, W.J., O'Brien, S., Makino, Y. and Poellinger, L. (1999) Regulation of the hypoxia-inducible transcription factor 1alpha by the ubiquitin-proteasome pathway. J. Biol. Chem. 274, 6519–6525.
[5] Bruick, R.K. and McKnight, S.L. (2001) A conserved family of prolyl-4-hydroxylases that modify HIF. Science 294, 1337–1340.
[6] Epstein, A.C., Gleadle, J.M., McNeill, L.A., Hewitson, K.S., O'Rourke, J., Mole, D.R., Mukherji, M., Metzen, E., Wilson, M.I., Dhanda, A., Tian, Y.M., Masson, N., Hamilton, D.L., Jaakkola, P., Barstead, R., Hodgkin, J., Maxwell, P.H., Pugh, C.W., Schofield, C.J. and Ratcliffe, P.J. (2001) *C. elegans* EGL-9 and mammalian homologs define a family of dioxygenases that regulate HIF by prolyl hydroxylation. Cell 107, 43–54.
[7] Cockman, M.E., Masson, N., Mole, D.R., Jaakkola, P., Chang, G.W., Clifford, S.C., Maher, E.R., Pugh, C.W., Ratcliffe, P.J. and Maxwell, P.H. (2000) Hypoxia inducible factor-alpha binding and ubiquitylation by the von Hippel-Lindau tumor suppressor protein. J. Biol. Chem. 275, 25733–25741.
[8] Ohh, M., Park, C.W., Ivan, M., Hoffman, M.A., Kim, T.Y., Huang, L.E., Pavletich, N., Chau, V. and Kaelin, W.G. (2000) Ubiquitination of hypoxia-inducible factor requires direct binding to the beta-domain of the von Hippel-Lindau protein. Nat. Cell Biol. 2, 423–427.
[9] Kamura, T., Sato, S., Iwai, K., Czyzyk-Krzeska, M., Conaway, R.C. and Conaway, J.W. (2000) Activation of HIF1alpha ubiquitination by a reconstituted von Hippel-Lindau (VHL) tumor suppressor complex. Proc. Natl. Acad. Sci. USA 97, 10430–10435.
[10] Tanimoto, K., Makino, Y., Pereira, T. and Poellinger, L. (2000) Mechanism of regulation of the hypoxia-inducible factor-1 alpha by the von Hippel-Lindau tumor suppressor protein. EMBO J. 19, 4298–4309.
[11] Harada, H., Hiraoka, M. and Kizaka-Kondoh, S. (2002) Antitumor effect of TAT-oxygen-dependent degradation-caspase-3 fusion protein specifically stabilized and activated in hypoxic tumor cells. Cancer Res. 62, 2013–2018.
[12] Kizaka-Kondoh, S., Inoue, M., Harada, H. and Hiraoka, M. (2003) Tumor hypoxia: a target for selective cancer therapy. Cancer Sci. 94, 1021–1028.
[13] Inoue, M., Mukai, M., Hamanaka, Y., Tatsuta, M., Hiraoka, M. and Kizaka-Kondoh, S. (2004) Targeting hypoxic cancer cells with a protein prodrug is effective in experimental malignant ascites. Int. J. Oncol. 25, 713–720.
[14] Harada, H., Kizaka-Kondoh, S. and Hiraoka, M. (2005) Optical imaging of tumor hypoxia and evaluation of efficacy of a hypoxia-targeting drug in living animals. Mol. Imaging 4, 182–193.
[15] Fernandes-Alnemri, T., Litwack, G. and Alnemri, E.S. (1994) CPP32, a novel human apoptotic protein with homology toaenorhabditis elegans cell death protein Ced-3 and mammalian interleukin-1 beta-converting enzyme. J. Biol. Chem. 269, 30761–30764.
[16] Iliopoulos, O., Kibel, A., Gray, S. and Kaelin Jr., W.G. (1995) Tumour suppression by the human von Hippel-Lindau gene product. Nat. Med. 1, 822–826.
[17] Johnson, C.R. and Jarvis, W.D. (2004) Caspase-9 regulation: an update. Apoptosis 9, 423–427.
[18] Nagarajah, N.S., Vigneswaran, N. and Zacharias, W. (2004) Hypoxia-mediated apoptosis in oral carcinoma cells occurs via two independent pathways. Mol. Cancer 3, 38.
[19] Mirnezami, A.H., Campbell, S.J., Darley, M., Primrose, J.N., Johnson, P.W. and Blaydes, J.P. (2003) Hdm2 recruits a hypoxia-sensitive corepressor to negatively regulate p53-dependent transcription. Curr. Biol. 13, 1234–1239.
[20] Zhu, Y., Mao, X.O., Sun, Y., Xia, Z. and Greenberg, D.A. (2002) p38 Mitogen-activated protein kinase mediates hypoxic regulation of Mdm2 and p53 in neurons. J. Biol. Chem. 277, 22909–22914.
[21] Alarcon, R., Koumenis, C., Geyer, R.K., Maki, C.G. and Giaccia, A.J. (1999) Hypoxia induces p53 accumulation through MDM2 down-regulation and inhibition of E6-mediated degradation. Cancer Res. 59, 6046–6051.
[22] Graeber, T.G., Peterson, J.F., Tsai, M., Monica, K., Fornace Jr., A.J. and Giaccia, A.J. (1994) Hypoxia induces accumulation of p53 protein, but activation of a G1-phase checkpoint by low-oxygen conditions is independent of p53 status. Mol. Cell. Biol. 14, 6264–6277.
[23] Soengas, M.S., Alarcon, R.M., Yoshida, H., Giaccia, A.J., Hakem, R., Mak, T.W. and Lowe, S.W. (1999) Apaf-1 and caspase-9 in p53-dependent apoptosis and tumor inhibition. Science 284, 156–159.
[24] Rothmann, T., Hengstermann, A., Whitaker, N.J., Scheffner, M. and zur Hausen, H. (1998) Replication of ONYX-015, a potential anticancer adenovirus, is independent of p53 status in tumor cells. J. Virol. 72, 9470–9478.
[25] Bouvet, M., Bold, R.J., Lee, J., Evans, D.B., Abbruzzese, J.L., Chiao, P.J., McConkey, D.J., Chandra, J., Chada, S., Fang, B. and Roth, J.A. (1998) Adenovirus-mediated wild-type p53 tumor suppressor gene therapy induces apoptosis and suppresses growth of human pancreatic cancer. Ann. Surg. Oncol. 5, 681–688.

Acta Oncologica, 2006; 45: 317–324

Taylor & Francis
Taylor & Francis Group

ORIGINAL ARTICLE

Suppression of VEGF transcription in renal cell carcinoma cells by pyrrole-imidazole hairpin polyamides targeting the hypoxia responsive element

YUKIO KAGEYAMA[1], HIROSHI SUGIYAMA[2,3], HIROHITO AYAME[2], AKI IWAI[1], YASUHISA FUJII[1], L. ERIC HUANG[4], SHINAE KIZAKA-KONDOH[5], MASAHIRO HIRAOKA[5] & KAZUNORI KIHARA[1]

[1]*Department of Urology, Graduate School of Tokyo Medical and Dental University, 1-5-45 Yushima, Bunkyo-ku, Tokyo, 113-8519, Japan,* [2]*Institute of Biomaterials and Bioengineering, Tokyo Medical and Dental University, 2-3-10 Surugadai, Kanda, Chiyoda-ku, Tokyo 101-0062, Japan,* [3]*Department of Chemistry, Graduate School of Science, Kyoto University, Kitashirakawa Oiwakecho, Sakyo-ku, Kyoto, 606-8502, Japan,* [4]*Laboratory of Human Carcinogenesis, NCI, National Institute of Health, Bethesda, MD, USA and* [5]*Department of Therapeutic Radiology and Oncology, Graduate School of Medicine, Kyoto University, 54 Kawahara-cho, Shogoin, Kyoto, 606-8507, Japan*

Abstract

Hypoxia inducible factor (HIF), a master regulator of critical genes for cell survival under hypoxic conditions, is known to be related to tumorigenesis and progression of renal cell carcinoma. *N*-methylpyrrole (Py)-*N*-methylimidazole (Im) hairpin polyamides are synthetic organic compounds that recognize and bind to the minor grooves of specific DNA sequences. We synthesized three Py-Im hairpin polyamides targeting the flanking sequences of hypoxia responsive element (HRE; a binding site of HIF) in the promoter region of the vascular endothelial growth factor (VEGF) gene. The effects of the polyamides on HIF-induced transcription were evaluated by a luciferase assay using a reporter plasmid containing a VEGF promoter. Real time reverse-transcriptase polymerase chain reaction and enzyme-linked immunosorbent assay were performed to examine the effects of the polyamides on the transcription and secretion of VEGF in A498 renal cell carcinoma cells, which have a frame-shift mutation in the von Hippel-Lindau gene. A combination of three Py-Im hairpin polyamides suppressed HIF-induced transcription in reporter assays using 293 cells and successfully suppressed transcription and translation of the VEGF gene in A498 cells. Inhibition of the HIF-HRE interaction was confirmed by an electrophoresis mobility shift assay. An approach using Py-Im hairpin polyamides may be a new strategy for the treatment of renal cell carcinoma.

Hypoxia inducible factor (HIF) is a key regulator of molecules that are critical to cell survival under hypoxic conditions [1]. In low-oxygen conditions, HIFs (HIF-1 or HIF-2 bind to the hypoxia responsive element (HRE), and trigger the transcription of target genes such as vascular endothelial growth factor (VEGF) or erythropoietin. Under normal oxygen tension, the von Hippel-Lindau (VHL) protein binds to the alpha subunits of the HIFs (HIF-1α or HIF-2α) and facilitates their rapid degradation.

Renal cell carcinoma is characterized by extensive neovascularization. Recently, frequent mutations of the VHL gene have been demonstrated in familial and sporadic renal cell carcinoma with clear cell phenotypes. Stabilization of HIFs due to an impaired VHL-HIF interaction has been shown to be an underlying mechanism of hypervascularity in renal cell carcinoma [2]. Thus, suppression of transcriptional activity of these HIFs may lead to decreases in de novo vascular formation and provide a new treatment modality for renal cell carcinoma that is resistant to radiation or chemotherapy.

N-methylpyrrole (Py)-*N*-methylimidazole (Im) hairpin polyamides have been shown to bind to the minor groove of specific DNA sequences with affinity and specificity similar to those of

Correspondence: Yukio Kageyama, Department of Urology, Graduate School of Tokyo Medical and Dental University, 1-5-45 Yushima, Bunkyo-ku, 113-8519 Tokyo, Japan. E-mail: kageyys.uro@tmd.ac.jp

(Received 15 September 2005; accepted 21 November 2005)

ISSN 0284-186X print/ISSN 1651-226X online
DOI: 10.1080/02841860500486648